

Multivariate Patterns of Age-Associated Microstructural Change Measured by Diffusion Kurtosis Imaging

Jean-Philippe Coutu^{1,2}, H. Diana Rosas², and David Salat^{2,3}

¹Health Sciences and Technology, Massachusetts Institute of Technology, Cambridge, MA, United States, ²MGH/HST Athinoula A. Martinos Center for Biomedical Imaging, MA, United States, ³VA Boston Healthcare System, MA, United States

INTRODUCTION: The idea that different pathologies affect specific diffusional properties preferentially [1,2] has potential value in the diagnosis and tracking of specific disease processes as opposed to more generic tracking of cumulative white matter damage without specific etiology. To date, however, little if any work has attempted to differentiate between various types of age-associated white matter changes based on multivariate diffusion properties. Although DTI provides multiple indices of diffusional behavior, it is possible that composite information across a wider range of diffusional processes beyond what DTI provides would enable better classification of differing patterns of white matter damage with aging and disease. Diffusional kurtosis imaging (DKI) is a recently developed neuroimaging technique [3] enabling the additional characterization of the tissue diffusional heterogeneity. The goal of our study was to use these novel diffusion metrics to determine whether DKI provides additional, unique information compared to DTI to identify different types of microstructural changes with aging.

METHODS: A total of 111 healthy adults between 33 and 91 years of age (62 women, 49 men) were imaged on a Siemens 3T Trio system (Erlangen, Germany) with a 32-channel head coil. Whole-brain diffusion-weighted scans were acquired (TR = 9250 ms, TE = 103 ms, 2 mm isotropic, 64 slices total, acquisition matrix 128 x 128, 6/8 partial Fourier, bandwidth = 1396 Hz/pixel, 24 non-collinear directions with b-values of 700, 1400 and 2100 s/mm², and 10 T2-weighted (b0) images with b-value = 0 s/mm²). The diffusion and diffusional kurtosis tensors were fitted using the FandTasia toolbox implemented in MATLAB [4,5] and then used to obtain the mean, axial and radial kurtosis (MK, AK and RK) maps, which were then median-filtered to remove potential outlying values. Maps of DTI metrics were obtained based on the first b-value of the DKI dataset. White matter tracts and subcortical regions on the TBSS [6] skeleton were segmented using a combination of FreeSurfer's T1-based white-matter parcellation and FSL's JHU white matter labels [7]. Mean DKI/DTI measures of the 46 bilateral ROIs were extracted in the native space of each individual, and correlated with age to obtain the age effect size of each DTI/DKI metric. The regions were then clustered using MATLAB's k-means clustering procedure based on their resulting age effect size profile.

RESULTS: K-means clustering was used on both DTI metrics alone and on DTI+DKI metrics to group regions with similar age effect sizes across metrics, based on two different measures of similarity: **(1) squared Euclidean distance:** clustered regions according to their overall degree of age effect size across metrics, and was unaffected by the addition of DKI metrics (Figure 1a and b). Clusters 1, 2 and 3 respectively resemble regions with low, medium and high relative-effect scores, and the average age effect size in each cluster confirmed this partition. This suggests that the greatest distinction between clusters seems to be their average age effect size across all diffusion metrics, and indicates that DKI metrics do not add any significant information in that respect. **(2) correlation:** clustered together regions with a similar pattern of relative metric-age effect sizes ('diffusion footprint') instead of the overall effect size (Figure 1c and d). Indeed, in Figure 1a, the center clusters all shared a similar diffusion footprint (relatively high RD- and low AD-age effect sizes, medium-high MD- and FA-age effect sizes). Most of these regions were therefore clustered together (cluster 1) in Figure 1c. Cluster 2 had few regions and was similar to cluster 1 except for a lower relative FA-age effect size, and cluster 3 represented regions driven mainly by a high increase in MD with age. A key observation is that the addition of DKI metrics split cluster 1 into two distinct clusters, shown by clusters 1 and 2 in Figure 1d. The main difference lied in the DKI metrics, with both DTI and DKI metrics having similar age effects in cluster 1, and DKI metrics having higher age effects in cluster 2. Regions from cluster 3 however were already properly clustered using DTI metrics only, and these regions exhibited mostly isotropic changes in diffusivity and diffusional kurtosis.

DISCUSSION: Initial clustering experiments were driven by the overall average age effects across all diffusion metrics, to which the addition of DKI metrics did not have a noticeable effect. However, our multivariate diffusion footprint clustering approach provided a more holistic view of the types of age effects on the diffusion microenvironment, and led to a quite different spatial pattern than that produced from the average age effect across diffusion metrics. For example, while the cerebellum and superior frontal white matter seem to undergo a similar type of microstructural changes, the superior frontal white matter undergoes a greater degree of these changes than the cerebellum. Furthermore, DKI metrics allowed a clustering that was not possible with DTI metrics alone.

CONCLUSION: DKI metrics were useful in combination with DTI metrics for the classification of regions according to their multivariate 'diffusion footprint', or pattern of relative age effect sizes. It is possible that the multivariate patterns of age-associated changes measured are representative of different types of microstructural pathology. These results suggest that DKI provides important complementary indices of brain microstructure for the study of brain aging and neurological disease.

REFERENCES: [1] Song et al. *Neuroimage* 2003;20(3):1714-22. [2] Song et al. *Neuroimage* 2002;17(3):1429-36. [3] Jensen et al. *Magn Reson Med* 2005;53(6):1432-40. [4] Barmpoutis and Vemuri. *Proc. IEEE Intl Symp Biomed Imaging* 2010:1385-88. [5] Barmpoutis and Zhuo. *8th IEEE Intl Symp on Biomed Imaging* 2011:262-5. [6] Smith et al. *Neuroimage* 2006;31(4):1487-1505. [7] Salat et al. *Neuroimage* 2012;59(1):181-92.

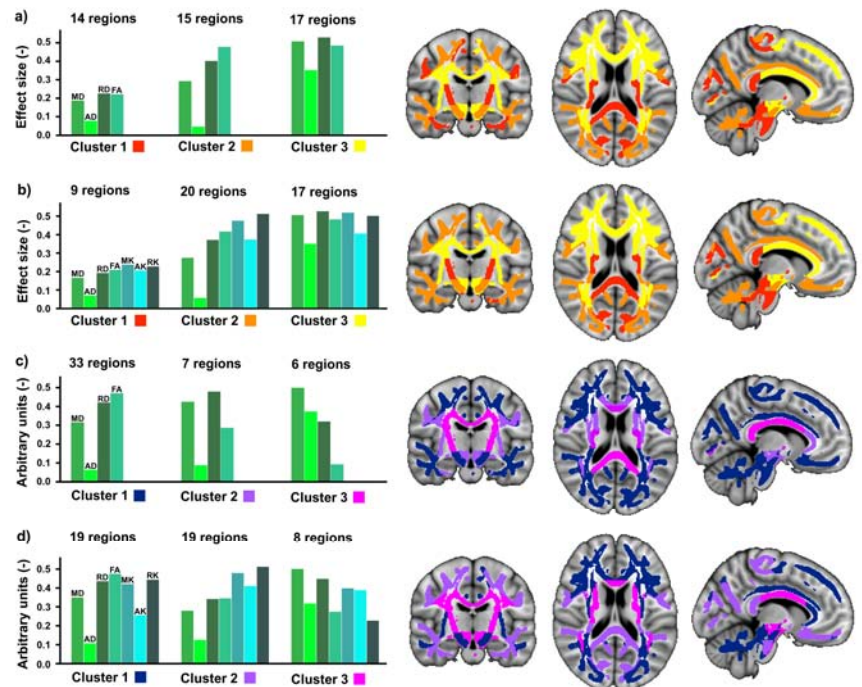


Figure 1 Results of the k-means clustering procedure using a squared Euclidean distance as similarity measure based on DTI metrics alone (a) and with DTI+DKI metrics (b). The age effect size of every diffusion metric is shown for each cluster center. The sign of the age effect size was inverted for FA, MK, AK and RK for clustering purposes. Results of the k-means clustering procedure using correlation as similarity measure based on DTI metrics alone (c) and with DTI+DKI metrics (d). In this case, regions in each cluster shared a diffusion footprint that was most highly correlated with the diffusion footprint of their cluster center, regardless of their overall age-association strength for all metrics. Arbitrary units are used to represent each cluster center as the diffusion footprint can be demeaned and scaled across metrics without changing its correlation coefficient with the diffusion footprint of each region. In every case, a representation of each region colored according to their classification is shown on the dilated TBSS skeleton for easier visualization (analyses were solely performed on the white matter skeleton). (MD/AD/RD: mean/axial/radial diffusivity; FA: fractional anisotropy; MK/AK/RK: mean/axial/radial kurtosis).